Natural Hazards (2024) 120:5509–5536
https://doi.org/10.1007/s11069-024-06431-5

ORIGINAL PAPER

Determination of land surface temperature and urban heat island effects with remote sensing capabilities: the case of Kayseri, Türkiye

Mehmet Cetin[1] · Mehtap Ozenen Kavlak[2] · Muzeyyen Anil Senyel Kurkcuoglu[3] · Gulsah Bilge Ozturk[4] · Saye Nihan Cabuk[5] · Alper Cabuk[6]

Received: 28 September 2023 / Accepted: 12 January 2024 / Published online: 15 February 2024

Abstract
Kayseri, a densely urbanized province in Türkiye, grapples with pressing challenges of air pollution and limited green spaces, accentuating the need for strategic urban planning. This study, utilizing Landsat 8 and Landsat 9 satellite imagery, investigates the evolution of land surface temperatures (LST) and urban heat island (UHI) effects in key districts—Kocasinan, Melikgazi, Talas, and Hacılar—between 2013 and 2022. This research has been complemented with an analysis of the Normalized Difference Vegetation Index (NDVI) and the Normalized Difference Built-Up Index (NDBI), exploring correlations among the LST, UHI, NDVI, and NDBI changes. The findings indicate that a significant portion (65% and 88%) of the study area remained unchanged with respect to the NDVI and NDBI differences. This research's findings reveal that a substantial portion (65% and 88%) of the study area exhibited consistency in the NDVI and NDBI. Noteworthy increases in the NDVI were observed in 20% of the region, while only 4% exhibited higher NDBI. Strikingly, the UHI displayed strong negative correlations with the NDVI and robust positive correlations with the NDBI. The LST changes demonstrated a reduced temperature range, from 21 to 51 °C in 2013, to 18 to 40 °C in 2022. Localized environmental factors, notably at the National Garden site, showcased the most significant temperature variations. Notably, the UHI exhibited strong negative correlations with the NDVI and strong positive correlations with the NDBI. The study's results emphasize the interplay among the NDBI, LST, and UHI and an inverse relationship with the NDVI and NDBI, LST, and UHI. These findings hold implications for urban planning and policymaking, particularly in the context of resilient and sustainable land use planning and the UHI mitigation. This research underscores the intricate interplay among the NDBI, LST, and UHI, highlighting an inverse relationship with the NDVI. These findings hold crucial implications for resilient and sustainable urban planning, particularly in mitigating the UHI effects. Despite limited vacant spaces in Kayseri, geospatial techniques for identifying potential green spaces can facilitate swift UHI mitigation measures. Acknowledging Kayseri's complex dynamics, future research should delve into the UHI responses to urban morphology and design, extending this methodology to analyze the UHI effects in other Turkish cities. This research contributes to a broader understanding of UHI dynamics and sustainable urban planning practices, offering valuable insights for policymakers, urban planners, and researchers alike.

Extended author information available on the last page of the article

Keywords Urban planning · Urban heat island · Land surface temperature · Normalized difference built-up index · Normalized difference vegetation index

1 Introduction

Rapid and continuous urbanization has several negative impacts, including the UHI phenomenon. Urban built-up areas absorb and re-radiate solar radiation while generating warmer surface temperatures than the surrounding rural areas. Research by Jabal et al. (2022) highlights the importance of satellite image processing, particularly spectral vegetation indices, in assessing changes in land cover, land use, and crop production in Iraq. In their work, they investigated the effects of climatic factors, particularly temperature and precipitation, on crop production in Iraq and emphasized the vulnerability of rainfed farmers to climate change, especially to changes in precipitation patterns and rising temperatures. Changes in rainfall patterns and rising temperatures due to climate change are discussed in the context of their detrimental effects on crops. They find that rice and wheat production was volatile between 2008 and 2020 due to certain factors, such as high humidity and pest damage, indicating challenges for Iraqi agriculture. Tian et al. (2021) draw attention to the increase in the impervious surface in cities, which causes the urban fabric to alter surface radiation, temperature, and moisture levels drastically. In addition, the causes of UHI can be listed as vast and dense masses of high urban buildings, the existence of heat-absorbing artificial materials and surfaces, decreased vegetation cover, human-originated heat release, disturbed urban ventilation, and air pollution (Rizwan et al. 2008; Gober et al. 2009; Steeneveld et al. 2011; Mirzaei 2015; Aleksandrowicz et al. 2017; Palme et al. 2017; He 2019).

A UHI has various economic and environmental drawbacks, including more energy requirements, pollution, and decreased air quality (Grimm et al. 2008; Chun and Guldmann 2014; Kim and Guldmann 2014; Lowe 2016), as well as health issues (Zhao et al. 2014; Venter et al. 2020). Increased mortality and morbidity and decreased outdoor thermal comfort are also the most reflected impacts of the UHI effect. Proliferated risks based on future projections on urbanization and urban population augmentation have accelerated the efforts and research on the UHI. In future, even higher temperatures will be experienced in cities compared to rural landscapes (Zoran et al. 2011; Li et al. 2019), which makes the detection and mitigation of a UHI even more critical.

Determining the intensity and spatial distribution of a UHI makes it possible to reveal the size and geographic location/clustering of the UHI-related risks. The land cover types in urban areas are considerable determinants of a UHI, and the relationship between LST and NDVI is a key indicator of land cover changes (Singh and Grover 2015). An LST is also one of the most used indices together with atmospheric temperature in determining the UHI (Eludoyin et al. 2014; Sheng et al. 2017; Sun et al. 2020; Taloor et al. 2021; Tian et al. 2021). Therefore, several studies have discussed the relationship between vegetation/land cover and a UHI and/or an LST. Zou et al. (2021) found that land cover types affect the interaction between a UHI and heat waves, while the UHI intensity tended to be higher in heat waves in more urbanized areas. Kadhim et al. (2022) studied landscape fragmentation in urban areas and highlight the various factors that contribute to this phenomenon, such as unplanned urbanization, recreational activities, and land use changes leading to an increase in LST and UHI intensity due to land transformation resulting from human activities and fragmentation. The study highlights the urgent need to assess landscape fragmentation,

especially in rapidly urbanizing areas such as Baqubah in Iraq. It uses innovative and feasible alternative techniques with multispectral Sentinel-2 imagery to assess urban expansion by analyzing landscape fragmentation instead of using conventional, non-cost-effective methods that are hampered by time constraints. Their novel method incorporates spatial indicators, machine learning classification, landscape fragmentation analysis, and an original approach to estimate future urban expansion paths, providing valuable information for decision-making and urban planning. Wang et al. (2016) concluded that urban expansion significantly impacted a UHI, and the temperature of the previously built-up areas tended to increase with new urban developments. Rousta et al. (2018) observed that an increase in the impervious surface and a decrease in vegetated land resulted in an LST increase between 1988 and 2018 in their study area. Yao et al. (2020) confirmed the cooling effect of urban green spaces while stating the importance of landscape configuration and composition. Based on these findings, a good number of UHI mitigation policies and strategies inevitably focus on relieving the adverse effects of a UHI and improving the quality of life while increasing the vegetation in urban areas (Mackey et al. 2012; Shishegar 2014; Norton et al. 2015; O'Malley et al. 2015; Sun et al. 2017; Taleghani 2018; Arghavani et al. 2020; Yao et al. 2020; Ke et al. 2021). Similarly, Ke et al. (2021) emphasized that urban green spaces have the potential for UHI mitigation, while the types of urban functional zones is important in different planning strategies for green areas. Vegetation, indeed, tends to have a cooling effect due to its relation to the earth's albedo and surface temperature (Adeyeri et al. 2017). Therefore, a number of studies suggest that the more extensive the vegetation cover, the better the urban cooling (Al-Saadi et al. 2020).

UHI studies commonly adopt remote sensing satellite imageries and simulation techniques (Rizwan et al. 2008; Sheng et al. 2017). Remote sensing thermal images, such as that of Landsat and MODIS (Weng et al. 2014; Bonafoni 2016; Liu et al. 2016; Bonafoni and Keeratikasikorn 2018; How Jin Aik et al. 2020), are generally used when retrieving the LST index. These data have several advantages due to their relatively lower costs and availability of long-time series (Tian et al. 2021). Satellite images from different satellites' sensors at various geographic resolutions have also been used to measure land cover changes with the implementation of NDVI analysis and relate these changes with LST. For example, Silva et al. (2018) conducted a study in Paço do Lumiar, Brazil, to detect the land cover changes between 1988 and 2014 using Landsat images and to evaluate the relations between the urban temperatures and built-up areas. The results indicated increased temperatures, especially in the built-up areas, some noticeable hotspots in the residential and commercial regions, and low temperatures in the vegetated lands. The authors reported that green areas help provide better outdoor thermal comfort and prevent heat waves in cities. Similarly, Grigoraș and Urițescu (2019) used Landsat 5, Landsat 7, and Landsat 8 images to apply supervised classification and NDVI techniques finding that land cover changes in Bucharest, Romania, between 1984 and 2016 impacted the urban surface temperatures. Lands transformed into built-up areas, and fallow lands were associated with the highest surface temperature increases. NDVI analysis findings revealed that the surface temperatures decreased as the density of the vegetation cover increased. In addition, Doi (2022) investigated passive cooling technologies in urban areas, especially in warm and tropical climates that are experiencing rapid urbanization, and examined their application and effectiveness in residential areas of Bangkok, Thailand. The study focuses on both new and old residential areas, analyzing the LST in February 2022, and assessing the impact of rooftop treatments on older buildings. The study shows that new residential areas benefit from passive cooling technologies and highlights their successful application. The results show that new residential areas are cooler than older ones, underlining the successful application of

passive cooling technologies. The study emphasizes the importance of continuous maintenance to maintain the cooling effect in urban environments and bridges the gap between theoretical knowledge and practical implementation. Mackey et al. (2012) evaluated the results of the urban cooling strategies implemented in Chicago, USA, between 1995 and 2010. 5 Landsat 5 image pairs, each pair with similar dates, capture time, and atmospheric conditions, were used by the authors to perform NDVI analyses, detect albedo values and relate them with the temperature. High-resolution aerial photography was used for the verification process. The results show that the temperature increase in Landsat images was inversely correlated with the increase in the NDVI and albedo. In other words, vegetation was found to have a more decreasing effect on the temperature than the non-vegetated albedo. Reflective roofs were also found to be strong implementations for cooling.

As mentioned in the above-given literature, the quantity of built-up areas is also significant and associated with LST. Therefore, the NDBI is used in addition to the NDVI, as an indicator in the UHI studies. In their study, Talukdar et al. (2022) used various land use indices derived from the Landsat datasets for 1991, 2001, and 2018 for Delhi and Mumbai. Their findings show that the NDVI had the highest impact on the UHI, and the NDBI had the highest impact on the LST, while the NDVI and NDBI had the highest spatial variation among all other indices. All indices except for the NDBI had a negative relationship with the UHI. Adeyeri et al. (2017) used Landsat 8 data while investigating UHI characteristics in Abuja, Nigeria, and stated that the NDBI and the modified NDVI are significant indicators of LST, while the former had a positive and the latter had a negative relationship with LST. Guha et al. (2018) utilized Landsat 5 and Landsat 8 imageries to reveal the UHI intensity in Florence and Naples regarding the relationship between the LST and two land cover indices, the NDVI and NDBI. They observed that the LST had a strong negative correlation with the former index and a strong positive correlation with the latter. Prasad and Singh (2022) analyzed the impact of green and built-up areas on the UHI with regard to the relationship between the LST, NDVI, and NDBI and confirmed the lower UHI in green areas due to higher NDVI and higher UHI in settled areas as a result of higher NDBI.

The literature already reveals the necessity of measuring the LST and the urban land cover to better understand and cope with the UHI impact. This study aims to determine the spatiotemporal changes in the LST and the UHI effect in the central districts of Kayseri, Türkiye between 2013 and 2022, focusing on the alterations in vegetated surfaces and built-up areas. Although the method used in the study is prevalent for such studies, the novel part of this research focuses on its implementation in the Kayseri district, which is a highly urbanized industrial city in Türkiye with a population of around 1.4 million and has become noticeable with its current landscape based planning and urban development implementations aiming to relieve the negative outcomes of high-density urbanization. In addition, extreme UHI values within the study area are also mapped and evaluated considering the ongoing urban park construction works in the city. The results are expected to support the planning approaches and efforts in the city. The study distinguishes itself from prior studies in the literature through several key aspects. Firstly, this research focuses specifically on the densely urbanized province of Kayseri in Türkiye, providing a localized analysis that addresses the unique challenges faced by this region. While existing studies may offer broader insight into UHI dynamics, this research narrows its scope to Kayseri, offering detailed observations and recommendations tailored to the local context. Secondly, the incorporation of Landsat 8 and Landsat 9 satellite imagery in the analysis sets this research apart. The utilization of these advanced remote sensing technologies allows for a more precise and up-to-date assessment of changes in LST and UHI effects over the study period (2013–2022). This enhances the accuracy and reliability of this research's findings

compared to studies that may rely on older or less sophisticated data sources. Furthermore, this study explores correlations among various factors, including the NDVI and the NDBI, providing a comprehensive understanding of the interplay between land cover changes, green infrastructure, and temperature variations. This integrative approach contributes to a more holistic view of the factors influencing UHI, distinguishing this study from studies that may focus on individual variables in isolation. Lastly, this study emphasizes the practical implications for urban planning and policymaking in Kayseri. By identifying specific locations, such as the National Garden site, experiencing significant temperature variations has been offered as actionable insight for targeted intervention. This application-oriented focus on sustainable land use planning and UHI mitigation strategies sets its work apart, providing valuable guidance for practitioners and decision-makers in Kayseri, and potentially serving as a model for similar urban contexts.

This study aims to determine the spatiotemporal changes in the UHI effect in the central districts of Kayseri, Türkiye, focusing on the alterations in vegetated surfaces and built-up areas. The LST is calculated to quantify the temperature in the study area and to develop the UHI maps for 2013 and 2022. Although the method used in the study is prevalent for such studies, the novel part of this study focuses on its implementation in the Kayseri district, which is a highly urbanized industrial city in Türkiye with a population of around 1.4 million and has become noticeable with its current landscape based planning and urban development implementations aiming to relieve the negative outcomes of high-density urbanization. In addressing the pressing challenges of urbanization in Kayseri, this study endeavors to fill a critical research gap by providing a comprehensive assessment of LST and UHI effects. While existing literature has explored similar themes, this research uniquely contributes by focusing on the central districts of Kayseri, Kocasinan, Melikgazi, Talas, and Hacılar, leveraging advanced remote sensing capabilities. The novelty of this research's approach lies in the meticulous analysis of the NDVI and the NDBI, unveiling correlations that shed light on the intricate dynamics between green spaces, built-up areas, and temperature variations. By delving into the specificities of Kayseri's urban morphology, this study not only addresses a distinct gap in the current literature, but also provides actionable insight for resilient and sustainable urban planning practices. As it has been navigated through the subsequent sections, the distinctiveness of this research's methodology, and its contributions to the broader understanding of UHI dynamics, will become increasingly evident. Additionally, extreme UHI values within the study area are also mapped and evaluated considering the ongoing urban park construction works in the city. The results are expected to support the planning approaches and efforts in the city to create a sustainable development.

2 Study area

The Kayseri province, Türkiye, is one of Anatolia's important industrial and trade centers. Kayseri is located in the southern part of central Anatolia and lies between the 370 45′ and 380 18′ northern latitudes and the 340 56′ and 360 59′ eastern longitudes (KTB 2022a). Kayseri is divided into sixteen districts and seventeen municipal regions (Kayseri İl Tarım ve Orman Müdürlüğü 2022; Kayseri Valiliği 2022a, b) with an overall population of 1,434,357 inhabitants, the area of the province is 16,917 km^2. Figure 1 shows the location of the study area.

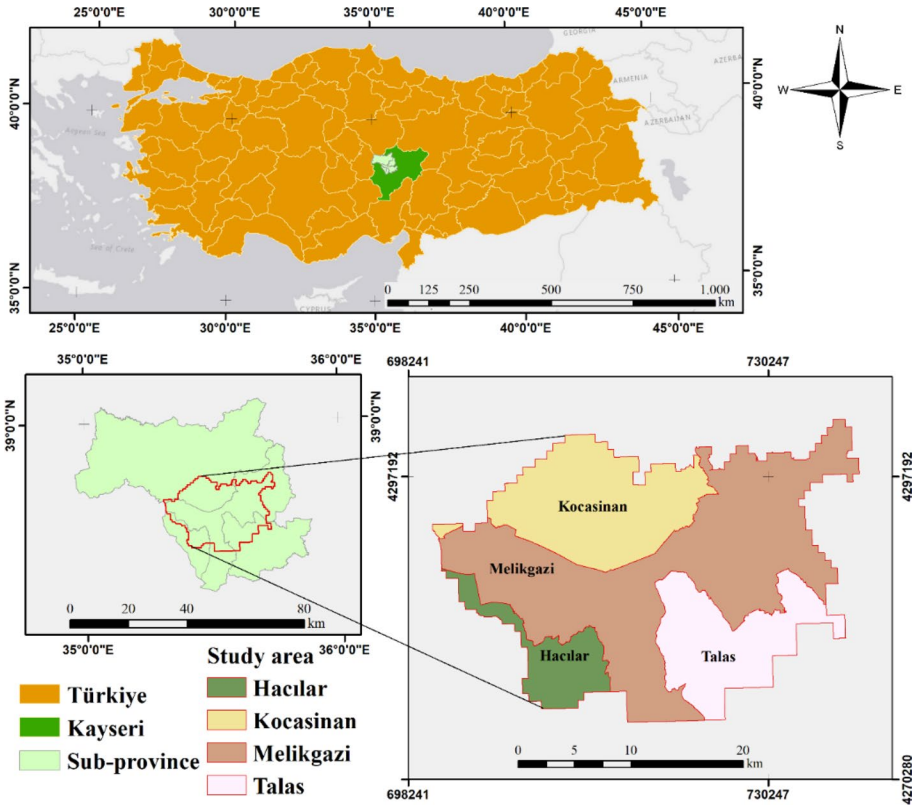

Fig. 1 Study area

The province's flora is mostly steppe, while 8% is covered with forests. Agricultural lands occupy approximately 40% of Kayseri's territories. The dominant climate is terrestrial, where hot and dry summers and cold and snowy winters prevail over the region. Summer temperatures reach up to 39.8 °C, and winter temperatures drop down to − 32.5 °C (Kayseri İl Tarım ve Orman Müdürlüğü 2022). In addition to its advanced industry, Kayseri province stands out in the country with its convenient transportation infrastructure, energy, and underground resources. Most citizens reside in urban centers and towns, and the rural population predominantly engages in agriculture (KTB 2022b).

Geographic thresholds played an important role in the city's macroform development. Agricultural areas in the north, the Erciyes mountain and natural and urban conservation areas in the south, wetlands in the southwest, and deep valley floors in the east, resulted in the city having a more compact-linear macroform that runs along the east–west axis. Kayseri has a long planning history, while five comprehensive plans, named after their leading planners, Burhan Çaylak (1936), Ölsner and Aru (1944), Yavuz Taşçı (1975), Topaloğlu and Berksan (1986), Bıyık and Doğan (2006), have directed the urban development over time (Kasap 2017). Plans considered a monocentric urban development with a strong Central Business District (CBD) connected to the rest of the city with large boulevards. Kayseri has a strong industrial basis, with three organized industrial zones and several other

small-scale industrial sites. The city primarily depends on automobiles, although tram lines run between the CBD and industrial, university, and mass housing areas.

Migration from rural areas caused unauthorized housing, although not as severe as in other Turkish cities due to the planned development. Topographic and natural thresholds, as well as mass migration, have paved the way for high densities in the city, while the built-up area has blocked the air corridors at the urban core. High levels of air pollution characterize the city due to the high-density urbanization and few green or open spaces. Air pollution is the most critical environmental issue in the city, according to the Environmental Problems and Priorities Report released by the Ministry of Environment and Urbanization (2020). In the 2020–2024 Strategic Plan prepared by the Kayseri Greater Municipality, it was indicated that green areas and urban parks remain insufficient due to intensive urbanization and high densities. Protecting the existing green spaces and increasing active green areas is determined as one of the thirty-seven strategic goals of the Strategic Plan to eliminate environmental problems, one of which is UHI.

3 Dataset

This study focuses on determining the UHI effect in the central districts of the Kayseri province, namely Kocasinan, Melikgazi, Talas, and Hacılar, covering an area of 641 km^2 (Fig. 1). The district borders were determined using the 2018 Urban Atlas data. The Urban Atlas data, produced from CORINE, include land cover/land use data of the cities with a population over 5000 for the EEA thirty-nine countries (EU28 + AFTA countries, Western Balkans, Türkiye) (Copernicus 2022).

The primary material of the study is the Landsat 8 and Landsat 9 satellite images obtained from the United States Geological Survey (USGS) database in GeoTIFF format. Table 1 gives information about the technical specifications of the images used in the study. Although the image resolution of the thermal band is 100 m, it is resampled and brought up to 30 m by the data provider before serving to users.

The study area borders were obtained in vector data format, and all the analyses and visualization processes were performed with ArcGIS 10.8.2 software.

4 Method

This study aims to determine the spatiotemporal changes in the UHI effects between 2013 and 2022 and their relationship with the changes in vegetated and built-up areas in the study area. Different methods to produce 3-staged outputs were utilized. The first stage is based on LST and UHI calculations, and during the second stage, NDVI and NDBI analyses were performed to determine the districts' vegetated and built-up regions. The final stage focuses on determining the correlations between the UHI, NDVI, and NDBI results. The workflow diagram regarding the method of the study is given in Fig. 2.

All the analyses were made using the Landsat 8, and Landsat 9 images (Table 1) captured on the closest dates for both years in August, which are reported as the rainless months with the highest temperatures in the Kayseri province (KTB 2022c). Images with cloud cover rates for each year are below 10%.

The below sections give detailed information regarding the methods of the study.

Table 1 Information about the satellite images used in the study

Date of image capturing	Name of the satellite	Bands used in the study	Wavelength (micrometers)	Resolution (meters)
12.08.2013	Landsat 8	Band 10—Thermal Infrared (TIRS) 1	10.6–11.19	100 (30)
		Band 4—Red	0.64–0.67	30
		Band 5—Near Infrared (NIR)	0.85–0.88	30
29.08.2022	Landsat 9	Band 10—Thermal Infrared (TIRS) 1	10.6–11.19	100 (30)
		Band 4—Red	0.64–0.67	30
		Band 5—Near Infrared (NIR)	0.85–0.88	30

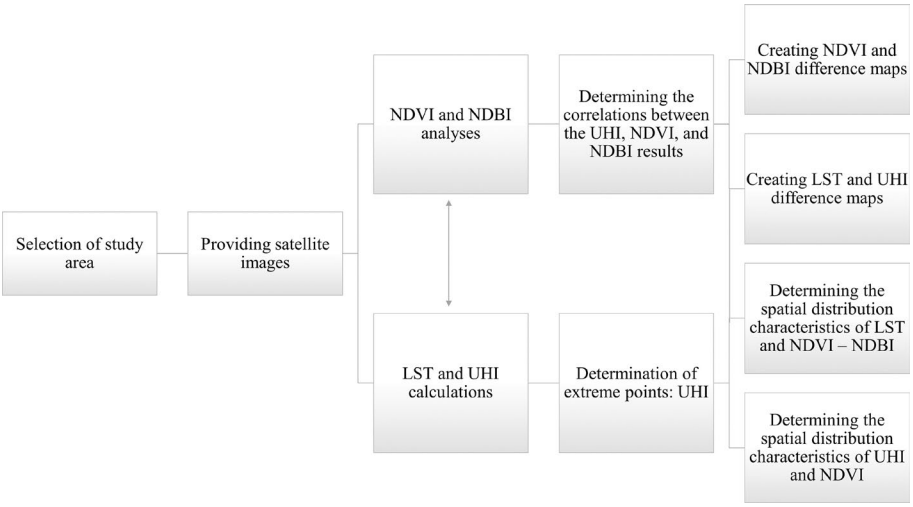

Fig. 2 Workflow chart

4.1 NDVI analysis

Plants absorb or reflect solar radiation and thereby impact surface temperature changes (Yuan et al. 2017). The relationship between NDVI and LST is quite complex and is, therefore, an important research area (Ghobadi et al. 2015).

NDVI is one of the significant indices defining the spectral change in the vegetation cover of an area (Khaliq et al. 2018). NDVI facilitates detecting the vegetated areas and evaluating the vegetation status. It is based on calculating the vegetation reflection values using near-infrared (NIR) and RED bands (Sun et al. 2021), which vary between − 1 and + 1 (Ozenen Kavlak et al. 2021). NDVI values closer to − 1 refer to unvegetated areas, values closer to 0 indicate sparse vegetation cover, and values closer to + 1 are associated with dense vegetation. Equation (1) below is used for calculating the NDVI values (Cetin et al. 2022).

$$\mathrm{NDVI} = (\mathrm{NIR} - \mathrm{RED})/(\mathrm{NIR} + \mathrm{RED}) \tag{1}$$

4.2 NDBI analysis

NDBI is one of the essential indices used to detect built-up areas. NDBI is obtained by dividing the difference between the spectral reflectance of short-wave infrared (SWIR) and NIR band values by their sum (He et al. 2010). The NDBI values range from + 1 to − 1. Positive NDBI values represent built-up areas, whereas non-urban or scattered built-up areas are represented by negative NDBI values (Zha et al. 2003). Values closer to -1 also represent water bodies or vegetation. The NDBI values are calculated using the formula in Eq. (2).

$$\mathrm{NDBI} = (\mathrm{SWIR} - \mathrm{NIR})/(\mathrm{SWIR} + \mathrm{NIR}) \tag{2}$$

Impermeable surfaces and structures (for example, buildings and roads) absorb solar radiation and reflect only a small portion. This situation causes higher temperatures in urban areas (Meng et al. 2022). The positive correlation between the NDBI and LST demonstrates that a built-up area significantly contributes to urban temperature rise since impermeable surfaces have a poor capacity to store water, which results in low humidity (Lu et al. 2009).

4.3 LST calculation

The LST is an essential parameter for detecting the relationship between the surface and atmosphere and for determining the UHI impact (Dickinson 1995; Zhou et al. 2011; Mallick et al. 2013). It is necessary to determine how thermal changes in urban areas affect the physical structure of cities and how it varies regarding surface morphology (Gupta et al. 2020; Liu et al. 2022). As infrared sensors in satellites measure radiances, which are inverted into temperature values with the application of different methods (Hall et al. 2008), thermal bands are commonly used in LST calculations. Band 10 is designated as Thermal Infrared (TIRS) 1 for Landsat 8 and 9 satellites. The LST calculation for Landsat 8 and 9 images requires the application of a five-step analysis series given in Table 2.

4.4 UHI calculation

The UHI is associated with increased artificial surfaces, energy use, and changes in industry and transportation due to population rise and unplanned urbanization (Izrael et al. 1990; Imhoff et al. 2010). These factors result in significant heat effects in urban areas compared to rural environments (Dousset and Gourmelon 2003; Vailshery et al. 2013), which can be calculated by Eq. (3) (Huang et al. 2019).

$$\mathrm{UHIER} = \Delta \mathrm{Ti}/\mathrm{Ts} = (\mathrm{Ti} - \mathrm{Ts})/\mathrm{Ts} \tag{3}$$

Here, UHIER is the intensity index of the UHI, Ti is the LST of the *i*-th pixel, and Ts is the mean LST of rural lands (Huang et al. 2019). The UHI intensity index results are based on the study of Huang et al. (2019) and are summarized in Table 3.

5 Results

This section gives the results obtained by applying the NDVI, NDBI, LST, and UHI analyses in the study area between 2013 and 2022.

5.1 NDVI and NDBI results

Figure 3 shows the distribution of the NDVI classes obtained for 2013 (Fig. 3a) and 2022 (Fig. 3b). The NDVI results were classified into five categories to reflect the intensity of the vegetation, where the lowest value refers to the unvegetated surfaces and the very high class is spared for the intensively vegetated areas. The results in both years show that low category regions dominate the study area covering over 75% of the districts for both years. Low vegetation is common in every direction except for the southwest parts, which mostly fall into the medium class. Table 4 gives the results of the NDVI analysis.

Table 2 The LST analyses and formula

Analysis	Formula	Definitions
Top of atmospheric reflectance (TOA) (Kumar et al. 2022)	$ML \times Q_{cal} + AL$	ML = Radiance multiplicative Band (No.10) AL = Radiance Add Band (No.10) Qcal = Quantized and calibrated standard product pixel values (DN)
TOA to brightness temperature (BT) conversion (Kumar et al. 2022)	$(K_2/\ln(K_1/L)+1)) - 273.15$	K_1 = Band-specific thermal conversion was constant from the metadata (774.8853) K_2 = Band-specific thermal conversion was constant from the metadata (1321.0789) L = TOA To obtain the results in Celsius, the radiant temperature is adjusted by adding the absolute zero (approx. − 273.15 °C)
Proportion of vegetation (P_V) (Kumar et al. 2022)	$((NDVI - NDVI_{min})/(NDVImax - NDVI_{min}))^2$	The minimum and maximum values of the NDVI image can be displayed directly in the image
Land surface emissivity (ε) (Kumar et al. 2022)	$0.004 * Pv + 0.986$	Pv = Proportion of vegetation The value of 0.986 corresponds to a correction value of the Equation
LST (Kumar et al. 2022)	$(BT/(1+(\lambda * BT/C2) * Ln(\varepsilon)))$ $(BT/(1+(0.00115 * BT/1.4388) * Ln(\varepsilon)))$	BT = Top of atmosphere brightness temperature (°C) λ = Wavelength of emitted radiance (0.00115) $C2 = h*c/s = 1.4388 \times 10–2$ mK = 14,388 mK h = Planck's constant = $6.626 \times 10–34$ J s s = Boltzmann constant = $1.38 \times 10–23$ JK c = Velocity of light = 2.998×108 m/s ε = Land surface emissivity

Table 3 The UHI intensity levels (Huang et al. 2019)

UHIER Value (Level ℃)	Level	Explanation
UHIER ≤ 0	Extremely low	Extreme low temperature zone (marginal LST difference between urban and rural areas)
0 < UHIER ≤ 0.1	Low	Low temperature zone (slight LST difference between urban and rural areas is slight)
0.1 < UHIER ≤ 0.2	Medium	Medium temperature zone (moderate LST difference between urban and rural areas)
0.2 < UHIER ≤ 0.3	High	High temperature zone (high LST difference between urban and rural areas)
0.3 < UHIER	Extremely high	Extreme high temperature zone (intensive LST difference between urban and rural areas)

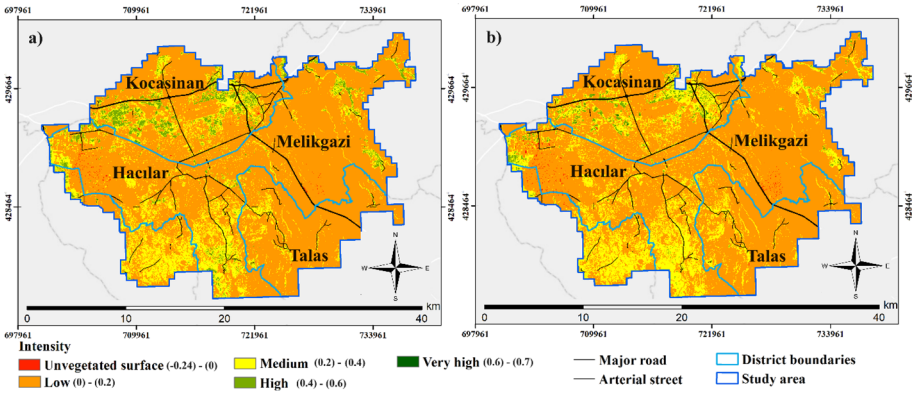

Fig. 3 **a** 2013 and **b** 2022 NDVI maps of the study area

Table 4 The NDVI analysis results

Vegetation Intensity	NDVI 2013		NDVI 2022	
	Percentage (%)	Area (km^2)	Percentage (%)	Area (km^2)
Unvegetated surface	0	1	0	2
Low	79	507	78	501
Medium	17	108	20	128
High	4	25	2	10
Very high	0	0	0	0
Total	100	641	100	641

The NDVI results for 2013 and 2022 do not reflect noticeable changes in the vegetation cover in the study area. Despite this, the areas classified as medium class show an increase from 17 to 20%, referring to an addition of 20 km^2, and the areas occupied by high class vegetation density are halved, referring to a loss of 10 km^2.

The NDBI results obtained for 2013 and 2022 are illustrated in Fig. 4. The NDBI results were also classified into five categories, from very high to very low, to reflect the intensity of the built-up areas. The NDBI analysis results are summarized in Table 5.

In 2013, the southeast parts of the study area hosted built-up areas classified under the very high category, whereas when the situation is reversed, the amount of very highly built-up areas showed a decrease of 29 km^2. Very low category seem to remain constant in terms of percentage and area, while the amount of built-up surfaces grouped under the low class is found to have increased by 12 km^2 in 2022.

When the NDVI and NDBI maps are compared, it can be observed that the built-up intensity in the study area decreases as the vegetation cover intensity increases. The increased built-up rate refers to the increased number of constructions and unvegetated lands. In addition, the difference maps for the NDVI and NDBI results were prepared to better understand how the study area changed between 2013 and 2022 in terms of vegetation cover and built-up lands (Fig. 5). In Fig. 5a, a noticeable change in the NDVI

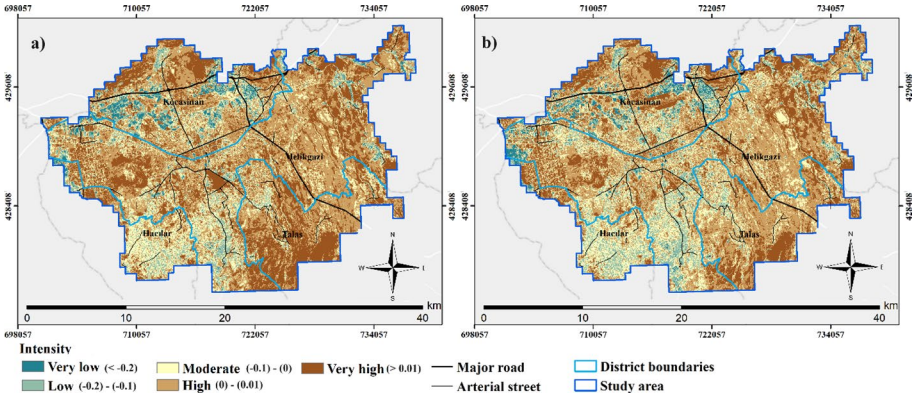

Fig. 4 **a** 2013 and **b** 2022 NDBI maps of the study area

Table 5 The NDBI analysis results

Built-up degree	NDBI 2013		NDBI 2022	
	Percent (%)	Area (km^2)	Percent (%)	Area (km^2)
Very low	2	16	2	16
Low	8	49	9	61
Moderate	18	118	21	136
High	41	265	41	263
Very high	30	194	26	165
Total	100	641	100	641

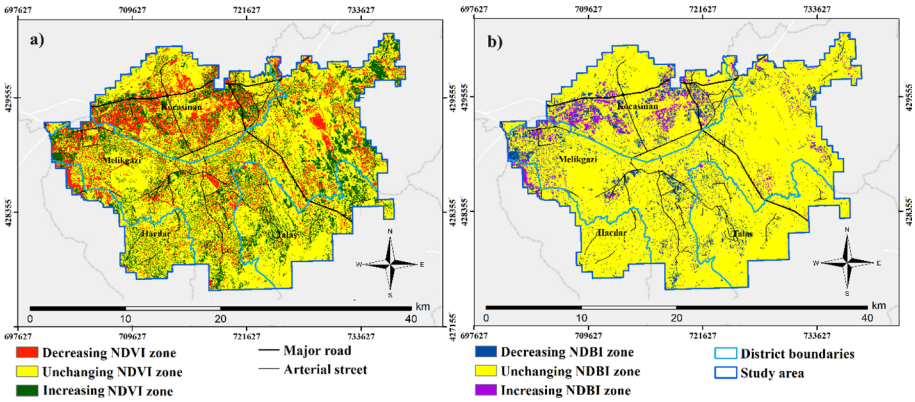

Fig. 5 **a** The NDVI and **b** NDBI difference maps for 2013 and 2022

results can be observed in the majority of the study area. Figure 5b shows that the NDBI changes are mainly in the northwest regions.

When the NDVI and NDBI difference maps are evaluated, the results show that the NDVI change ratio between 2013 and 2022 is higher than that of the NDBI (Table 6). The

Table 6 NDVI and NDBI difference results

	NDVI difference (2013–2022)			NDBI difference (2013–2022)		
	Pixel	Percent (%)	Area (km^2)	Pixel	Percent (%)	Area (km^2)
Decreasing zone	106,605	15	96	50,612	7	46
Unchanging zone	460,441	65	414	630,750	88	568
Increasing zone	145,726	20	131	31,410	4	28
Total	712,772	100	641	712,772	100	641

NDVI increase is observed in 20% of the study area, while a decrease is detected in 15% of the study area. On the other hand, the increase rate is only around 4% for the NDBI, and 7% of the study area has undergone an increasing trend. Decreases in the NDVI zone and increases in the NDBI zone mostly occupy the northern parts of the study area resulting from the intensive land use changes, including the development of a small industry site, a shopping mall, and a city hospital followed by the construction of residential units.

5.2 The LST and UHI results

The LST and UHI maps are illustrated in Figs. 6 and 7. According to Fig. 6, the LST values in 2013 range from 21 to 51 °C (Fig. 6a), while they vary between 18 and 40 °C in 2022 (Fig. 6b). On the other hand, in 2013, the UHI effect, which is classified into five classes, is extremely low in 89% of the study area. 10% of the area is exposed to medium UHI intensity and 1% to high UHI effects (Fig. 7a). In 2022, 49% of the study area is classified under the extremely low, 35% low, 15% medium, and 1% high UHI effect categories (Fig. 7b). According to these results, the 7% decrease in the low UHI regions between 2013 and 2022 can be explained by the increase seen in the extremely low (2%) and medium (5%) UHI classes.

The LST and UHI difference maps between 2013 and 2022 are shown in Fig. 8. Figure 8a reflects an extreme decrease in the LST in the majority of the study area, and

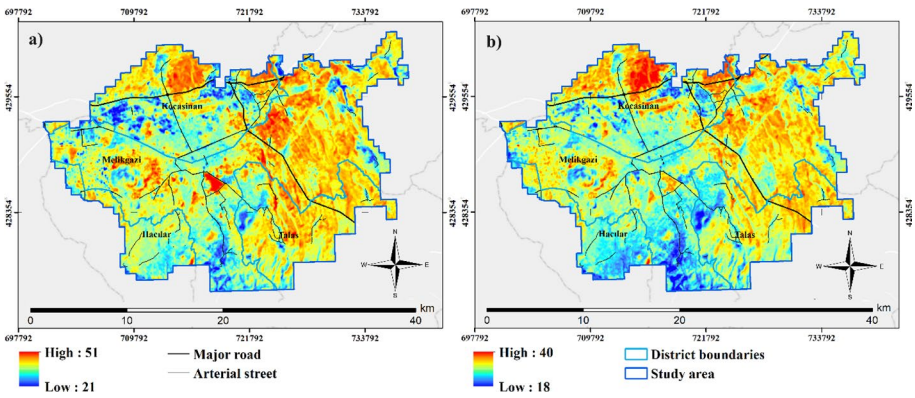

Fig. 6 **a** 2013 and **b** 2022 LST (°C) maps of the study area

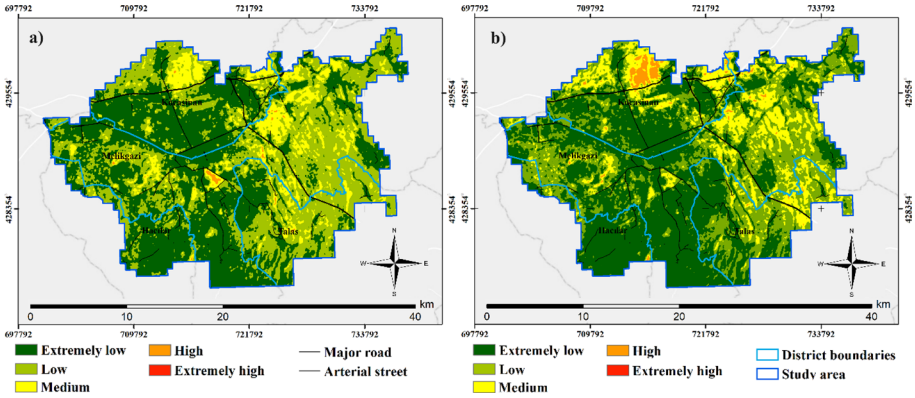

Fig. 7 **a** 2013 and **b** 2022 UHI maps of the study area

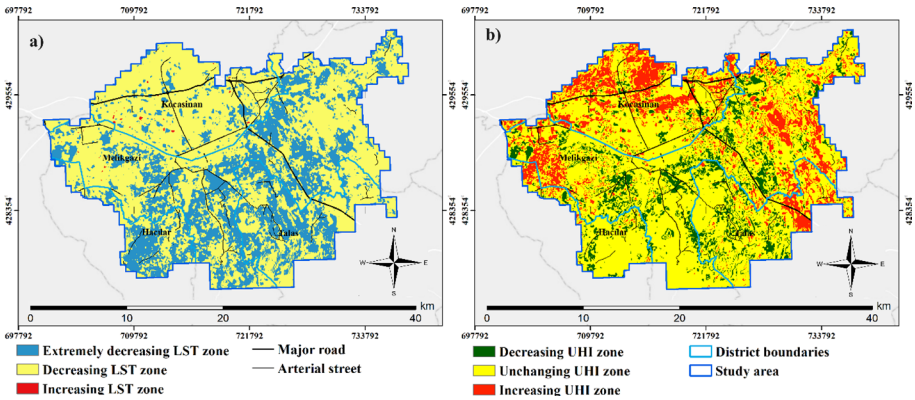

Fig. 8 LST (°C) (**a**) and UHI (**b**) difference maps for 2013 and 2022

Table 7 The LST and UHI difference results

	LST difference (°C) (2013–2022)			UHI difference (2013–2022)		
	Pixel	Percent (%)	Area (km^2)	Pixel	Percent (%)	Area (km^2)
Decreasing zone	234,360	33	211	82,727	12	74
Unchanging zone	477,658	67	430	513,747	72	462
Increasing zone	754	0	1	116,298	16	105
Total	712,772	100	641	712,772	100	641

Fig. 8b illustrates that the UHI change increases primarily in the northwest and western parts of the study area. The inner and southeastern parts have undergone a negative UHI change.

Table 7 shows that the total change in the LST between 2013 and 2022 is higher than that of the UHI. There is a negative change in the LST in 33% of the study area; this rate

is determined as 12% in the UHI. Additionally, 16% of the area has experienced a UHI increase.

Correlations between the UHI and NDVI, and the UHI and NDBI are − 0.591 and 0.588, and − 0.564 and 0.563, respectively, in 2013 and 2022 which verify that the UHI is negatively related to the NDVI and positively related to the NDBI.

5.3 Determination of extreme points: UHI

In this study, the results of the UHI analyses performed for 2013 and 2022 (Fig. 7) were further evaluated to detect the high and extremely high UHI zones (Fig. 9). The detected location represents the area that had a noticeably high UHI value in 2013 and which experienced a significant decrease in 2022. This location is covered within the boundaries of the Kayseri National Garden construction site, which is further discussed in the Discussions section of the study.

6 Results

The findings indicate that in Kayseri, the values of land conditions are based on the bare lands, rocks, residential areas, fields, and LST. According to these findings, there is a strong correlation between an increase in the LST and a rise in the UHI. To understand the relationship between each parameter, a comparison is also needed. This study examines how the NDVI, NDBI, LST, and UHI relate to one another and to the environment. Maps and graphs are used to display the results in the previous section.

It is found that variations in the different characteristics of the LULC's cause variations in the distribution of the LST. While the concrete surfaces cause high temperatures, the vegetated areas are directly linked to the lower surface temperatures cooling the urban microclimate. However, the LST does reach 51 °C in a few isolated areas of the site, which represent densely built-up areas or barelands. The highest surface temperatures in the city in 2013 coincided with the Kayseri Airlift Control Center, where the National Garden was to be built.

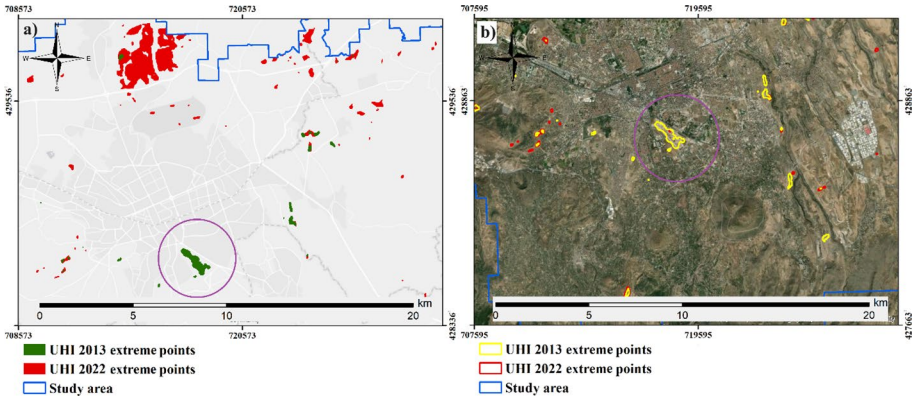

Fig. 9 Extreme UHI points for (**a**) 2013 and (**b**) 2022 (Circled areas show extreme UHI change locations in Kayseri National Garden that are further analyzed to develop stack profile)

70% of the Kayseri National Garden construction, which began in 2019, had been completed by 2022, according to Kayseri Büyükşehir Belediyesi (2019). The study results indicate that the Kayseri National Garden, located in the heart of Kayseri, already had a positive effect on the UHI effect during its construction phase in 2022. This positive effect was felt in a number of parts of its immediate surroundings and the city center. When analyzing the study's findings, it becomes clear how the microclimate in built environments and open green spaces changes with the LST and UHI values. While the microclimatic changes in built environments are most noticeable as temperature increases, this effect is transformed into an increase in thermal comfort in open spaces and nearby urban areas. Consequently, the results of this study show that green spaces in the study area in the four central districts of the province of Kayseri have a cooling effect on the thermal environment; therefore, these areas could reduce discomfort in metropolitan areas.

The NDVI, NDBI, LST, and UHI maps for 2013 are given in Fig. 10. Within the circled areas, the values for the NDBI, LST, and UHI increase in areas with low NDVI. This was particularly noted in 2013 when the NDVI levels were at their lowest and the NDBI, LST, and UHI were at their highest. In this context, the results show an inversely proportional relationship between the NDVI and the NDBI, LST, and UHI. The results of previous studies also presented the same relationship. Karnieli et al. (2010) and Lottering et al. (2022)

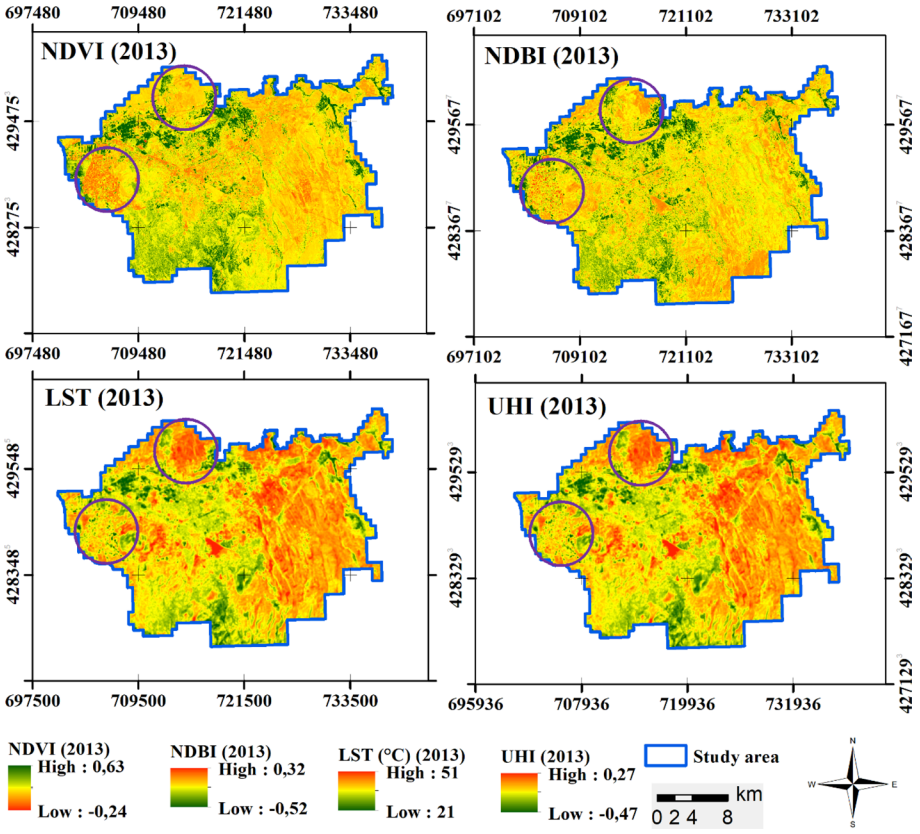

Fig. 10 2013 analysis maps

also presented the same results in their study areas. In addition to this, there is a directly proportional relationship among the NDBI, LST, and UHI. As previously mentioned in the results, a negative correlation between the UHI and NDVI and a positive correlation between the UHI and NDBI were detected, addressing that the UHI is negatively related to the NDVI and positively related to the NDBI. However, Macarof and Statescu (2017) note that this result of the NDVI negative relationship may vary by season, as vegetation cover changes seasonally. In summary, the NDBI is an accurate indicator of surface UHI effects and can be used as a complementary metric to the traditionally used NDVI.

6.1 Relationship between the LST-UHI and the NDVI-NDBI

Construction of Kayseri National Garden began in 2020, and 70% of it had been completed by 2022. A comparison of the NDVI and NDBI maps reveals that as the intensity of the vegetation cover increases, so does the study area's development. The increased built-up rate refers to the growth in the number of buildings and bare ground. The results also show a significant change in the LST and UHI between 2013 and 2022. The percentage of negative change in the LST (33%) is higher than in the study area's UHI (12%). A thorough investigation has been conducted into the causes of the extreme decline seen in the LST and UHI in 2022 (Fig. 11a). Profile line 1 and Profile line 2 were formed for the National Garden construction area in 2013, vertically crossing the boundaries of the high UHI zone

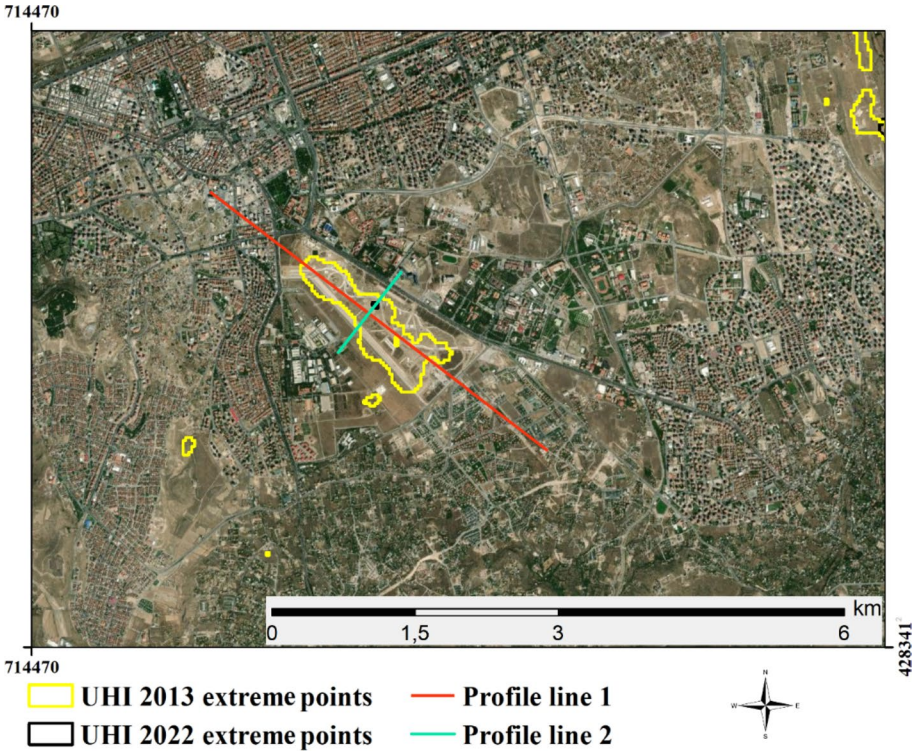

Fig. 11 Stack profile analysis map (UHI extreme points with profile lines)

(Fig. 11b). In the following parts, the spatial distribution characteristics of the NDVI, NDBI, LST, and UHI analyzes, and their relationships are investigated performing a stack profile analysis.

6.1.1 Spatial distribution characteristics of the LST and NDVI-NDBI

The distribution of the NDVI, NDBI, LST, and UHI has been evaluated using satellite data (Fig. 12). The correlation between the LST and NDVI is negative. A positive correlation between the LST and NDBI, which suggests that the built-up area may actually amplify the effects of the UHI, was found in contrast to the NDVI.

Considering the relationship between the LST, UHI, NDVI and NDBI, a direct relationship is expected between the LST, UHI and NDBI and an inverse relationship between the LST, UHI and NDBI and NDVI (Guha et al. 2018). In Fig. 12, the inverse relationship between the LST and NDBI in profile line 2, 400–440 m is remarkable (Fig. 12d). This situation was identified as a result of the detection of the extreme values of the UHI effect (Fig. 13a). In 2013, this area consisted entirely of bare land (Fig. 13b), while in 2022 the park began to take shape in this area, and the outlines of the areas that had begun to be built and greened became visible (Fig. 13c). For this reason, the NBDI values increase and decrease from time to time. This situation has also affected the LST. The extreme point of the UHI 2022 in this region has a different effect from the characteristics of the surrounding area, causing fluctuations in the graphs.

6.1.2 Spatial distribution characteristics of the UHI and NDVI

Mean LSTs for all land uses, and cover types between vegetated and non-vegetated areas differ significantly (Fig. 14). As an illustration, the distribution of parks and other green spaces within cities contributes to a decrease in the effect of the UHI and an improvement in the urban thermal environment. However, compared to the other types of land use and cover, agriculture had mean NDVI values that were significantly lower, except for parks and green areas. This indicates no significant differences in the NDVI between agricultural

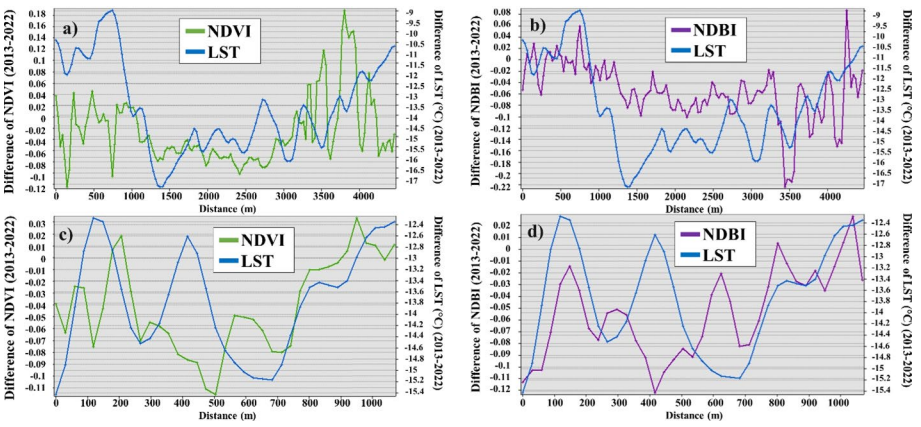

Fig. 12 LST and NDVI-NDBI stack profile graphs showing (**a**) Difference of NDVI and LST, (**b**) Difference of NDBI and LST, (**c**) Difference of NDVI and LST, (**d**) Difference of NDBI and LST

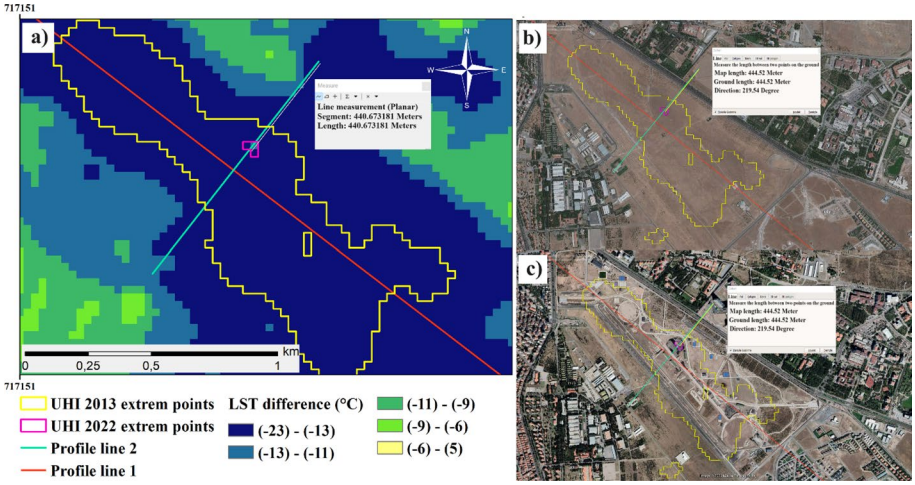

Fig. 13 Effects of extreme UHI points on stack profile graphics showing (**a**) Effect of UHI 2022 extreme point in LST and NDBI stack profile graph, (**b**) Kayseri National Garden (2013), (**c**) Kayseri National Garden (2022)

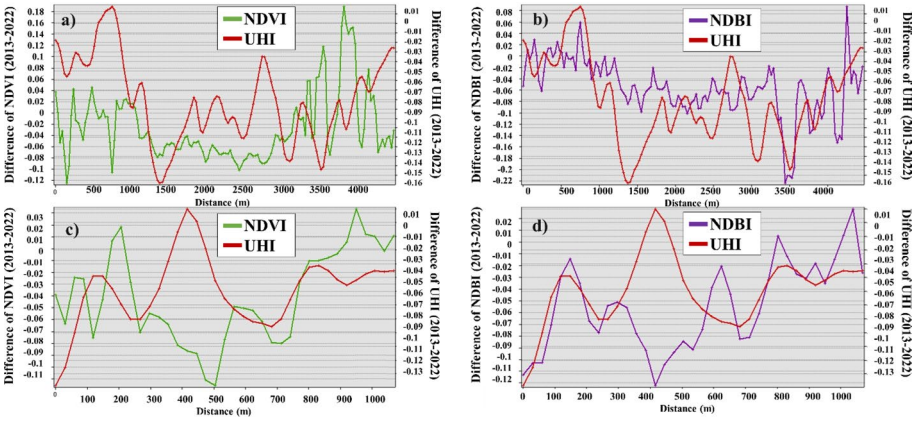

Fig. 14 UHI and NDVI-NDBI stack profile graphs

land and park/green space. However, due to differences in geographic location and the UHI effects, the mean LST values between the two LULC categories differ.

7 Discussion

To provide context for the research findings, this work's results were compared to existing studies on UHI dynamics. The observed negative correlations between the UHI and the NDVI, along with the positive correlations with the NDBI, align with prior research (Zha et al. 2003; Vailshery et al. 2013). However, this study offers a nuanced understanding

specific to the urban fabric of Kayseri, shedding light on unique temperature variations within its central districts. The decrease in LST range from 2013 to 2022 is consistent with global trends associated with green infrastructure improvements (Venter et al. 2020). Comparing this research's results to those of studies such as Jabal et al. (2022), underscores the distinctiveness of this research focus on a densely urbanized region, offering insight crucial for effective UHI mitigation strategies in similar contexts. This comparative analysis enhances the scientific value of this work, positioning it within the broader landscape of urban climate studies.

The theoretical implications of this manuscript extend beyond the specific context of Kayseri, Türkiye, to contribute valuable insight into the broader field of urban climate studies. By examining the interplay between LST, UHI effects, NDVI, and NDBI, this study sheds light on the intricate dynamics of temperature variations in densely urbanized areas. The observed correlations between the UHI and NDVI, coupled with the inverse relationship with the NDBI, emphasize the importance of green infrastructure in mitigating the UHI effects. This research's findings underscore the significance of considering local environmental factors and land use patterns in temperature distribution. This has implications for resilient and sustainable land use planning, offering guidance for urban planners in Kayseri and similar cities facing challenges of limited green spaces and high population density. Furthermore, the methodology employed in this study provides a template for analyzing the UHI effects in other urban contexts, contributing to a more comprehensive understanding of urban climate dynamics and informing future research endeavors in the field.

The practical implications of this manuscript are significant for urban planning and policy development, particularly in the context of Kayseri, Türkiye. The identified correlations between the LST, the UHI effects, the NDVI, and the NDBI offer practical insight for mitigating the impact of UHI in densely populated and urbanized areas. The observed negative correlations between the UHI and NDVI, along with the positive correlations with the NDBI, highlight the role of green infrastructure in moderating temperature variations. Urban planners in Kayseri can use geospatial information techniques to identify potential green spaces, strategically implementing measures to counteract the UHI effects. The temperature distribution patterns revealed in the study, influenced by specific local environmental factors, guide planners in identifying priority areas for intervention. The study's approach can be extended to other cities facing similar challenges, providing a practical template for assessing and addressing the UHI dynamics in the pursuit of sustainable and resilient urban development.

8 Conclusions

Based on the research that has been conducted, the results show significant changes in the UHI in the four central districts of the province of Kayseri, and that the local environment influenced the temperature distribution. Temperature changes based on the LST indicate a decline in the study area from 21 to 51 °C in 2013 to 18 to 40 °C in 2022. The specifics of the site affected how temperatures varied at different locations. The National Garden site is where the largest variations are thought to have occurred during the study period. There was a directly proportional relationship among the NDBI, LST, and UHI and an inversely proportional relationship between the NDVI and NDBI, LST, and UHI. Indices such as the NDVI, NDBI, LST, and other parameters may also impact

the UHI effect, and this study focuses on the extreme UHI points and how they vary when there is green space in urban areas.

This paper investigates the relationships between the UHI and the LST, the NDBI and the NDVI in Kayseri. The findings reveal a strong negative correlation between the LST and NDVI and a strong positive relationship between the LST and NDBI. Regarding resilient and sustainable land use planning and UHI mitigation, this study may be helpful for urban planning and policymaking. Although there are not many vacant spaces in Kayseri, using geospatial information techniques to pinpoint potential locations for green space planning can help researchers and urban planners act quickly to mitigate the UHI. As Kayseri exhibits complex dynamics in terms of both physical and demographic factors, it is advised that future research examine the UHI dynamics in response to urban morphology and design. The same method could be applied to other cities in the country.

In conclusion, this study illuminates crucial aspects of the LST dynamics and the UHI effects within the central districts of Kayseri, Türkiye, spanning the period from 2013 to 2022. The examination of satellite imagery, particularly Landsat 8 and Landsat 9 data, enabled a detailed assessment of temperature changes and UHI patterns, showcasing a notable decrease in the temperature range over the study area. This research's findings reveal significant correlations between the UHI, the NDVI, and the NDBI, emphasizing the intricate relationship between land cover changes, green infrastructure, and temperature variations. Importantly, the study identifies specific areas, exemplified by the National Garden site, experiencing pronounced temperature fluctuations, suggesting targeted intervention for effective urban planning and UHI mitigation. By addressing the local context of Kayseri, a nuanced understanding of the UHI dynamics is provided, offering actionable insight for sustainable land use planning in a densely urbanized region. In light of the research gaps filled and the novel contributions made, this study not only advances the scientific understanding of the UHI but also provides practical implications for policymakers and urban planners. The concise and focused nature of this research's conclusion distills the key findings, underscoring their significance and guiding future research and intervention in the realm of urban environmental management.

Acknowledgements This article was produced through cooperation between Başarsoft and Eskişehir Technical University under the TUBİTAK 2244 project number 119c200, executed by Prof. Dr. Alper Çabuk/Eskisehir Technical University.

Author contributions All authors contributed to the study conception and design. Material preparation, data collection and analysis were performed by Mehtap Özenen-Kavlak and Saye Nihan Çabuk. The first draft of the manuscript was written by Müzeyyen Anıl Şenyel Kürkçüoğlu, Gülşah Bilge Öztürk, Alper Çabuk, and Mehmet Cetin, and all authors commented on previous versions of the manuscript. All authors read and approved the final manuscript.

Funding Open access funding provided by the Scientific and Technological Research Council of Türkiye (TÜBİTAK). This article was produced through cooperation between Başarsoft and Eskişehir Technical University under the TUBİTAK 2244 project number 119c200, executed by Prof. Dr. Alper Çabuk/Eskisehir Technical University.

Data availability The data of the study will be provided upon request.

Code availability The materials of the study will be provided upon request.

Declarations

Conflict of interest The authors declare that they have no known competing financial interests or personal

relationships that could appear to influence the work reported in this paper.

Ethical approval Not applicable.

Consent to participate and consent to publish All authors agree with the content and all have given explicit consent to submit.

References

Adeyeri O, Akinsanola A, Ishola K (2017) Investigating surface urban heat island characteristics over Abuja, Nigeria: relationship between land surface temperature and multiple vegetation indices. Remote Sens Appl Soc Environ 7:57–68. https://doi.org/10.1016/j.rsase.2017.06.005

Aleksandrowicz O, Vuckovic M, Kiesel K, Mahdavi A (2017) Current trends in urban heat island mitigation research: observations based on a comprehensive research repository. Urban Clim 21:1–26. https://doi.org/10.1016/j.uclim.2017.04.002

Al-Saadi LM, Jaber SH, Al-Jiboori MH (2020) Variation of urban vegetation cover and its impact on minimum and maximum heat islands. Urban Clim 34:100707. https://doi.org/10.1016/j.uclim.2020.100707

Arghavani S, Malakooti H, Bidokhti A-AAA (2020) Numerical assessment of the urban green space scenarios on urban heat island and thermal comfort level in Tehran Metropolis. J Clean Prod 261:121183. https://doi.org/10.1016/j.jclepro.2020.121183

Bonafoni S (2016) Downscaling of Landsat and MODIS land surface temperature over the heterogeneous urban area of Milan. IEEE J Sel Top Appl Earth Obs Remote Sens 9(5):2019–2027. https://doi.org/10.1109/JSTARS.2016.2514367

Bonafoni S, Keeratikasikorn C (2018) Land surface temperature and urban density: multiyear modeling and relationship analysis using MODIS and Landsat data. Remote Sens 10(9):1471. https://doi.org/10.3390/rs10091471

Cetin M, Isik Pekkan Ö, Ozenen Kavlak M, Atmaca I, Nasery S, Derakhshandeh M, Cabuk SN (2022) GIS-based forest fire risk determination for Milas district, Turkey. Nat Hazards. https://doi.org/10.1007/s11069-022-05601-7

Chun B, Guldmann J-M (2014) Spatial statistical analysis and simulation of the urban heat island in high-density central cities. Landsc Urban Plan 125:76–88. https://doi.org/10.1016/j.landurbplan.2014.01.016

Copernicus (2022) Urban atlas. Copernicus. https://land.copernicus.eu/local/urban-atlas. Accessed 29 Oct 2022

Dickinson R (1995) Satellite systems and models for future climate change. World Surv Climatol 16:245–279

Doi R (2022) Are new residential areas cooler than older ones? Emerg Sci J 6(6):1346–1357. https://doi.org/10.28991/ESJ-2022-06-06-08

Dousset B, Gourmelon F (2003) Satellite multi-sensor data analysis of urban surface temperatures and land-cover. ISPRS J Photogramm Remote Sens 58(1–2):43–54. https://doi.org/10.1016/S0924-2716(03)00016-9

Eludoyin OM, Adelekan IO, Webster R, Eludoyin AO (2014) Air temperature, relative humidity, climate regionalization and thermal comfort of Nigeria. Int J Climatol 34(6):2000–2018. https://doi.org/10.1002/joc.3817

Ghobadi Y, Pradhan B, Shafri HZM, Kabiri K (2015) Assessment of spatial relationship between land surface temperature and landuse/cover retrieval from multi-temporal remote sensing data in South Karkheh Sub-basin. Iran Arab J Geosci 8(1):525–537. https://doi.org/10.1007/s12517-013-1244-3

Gober P, Brazel A, Quay R, Myint S, Grossman-Clarke S, Miller A, Rossi S (2009) Using watered landscapes to manipulate urban heat island effects: how much water will it take to cool Phoenix? J Am Plan Assoc 76(1):109–121. https://doi.org/10.1080/01944360903433113

Grigoraş G, Urițescu B (2019) Land use/land cover changes dynamics and their effects on surface urban heat island in Bucharest, Romania. Int J Appl Earth Obs Geoinf 80:115–126. https://doi.org/10.1016/j.jag.2019.03.009

Grimm NB, Faeth SH, Golubiewski NE, Redman CL, Wu J, Bai X, Briggs JM (2008) Global change and the ecology of cities. Science 319(5864):756–760. https://doi.org/10.1126/science.1150195

Guha S, Govil H, Dey A, Gill N (2018) Analytical study of land surface temperature with NDVI and NDBI using Landsat 8 OLI and TIRS data in Florence and Naples city. Italy Eur J Remote Sens 51(1):667–678. https://doi.org/10.1080/22797254.2018.1474494

Gupta N, Mathew A, Khandelwal S (2020) Spatio-temporal impact assessment of land use/land cover (LU-LC) change on land surface temperatures over Jaipur city in India. Int J Urban Sustain Dev 12(3):283–299. https://doi.org/10.1080/19463138.2020.1727908

Hall DK, Box JE, Casey KA, Hook SJ, Shuman CA, Steffen K (2008) Comparison of satellite-derived and in-situ observations of ice and snow surface temperatures over Greenland. Remote Sens Environ 112(10):3739–3749. https://doi.org/10.1016/j.rse.2008.05.007

He B-J (2019) Towards the next generation of green building for urban heat island mitigation: zero UHI impact building. Sustain Cities Soc 50:101647. https://doi.org/10.1016/j.scs.2019.101647

He C, Shi P, Xie D, Zhao Y (2010) Improving the normalized difference built-up index to map urban built-up areas using a semiautomatic segmentation approach. Remote Sens Lett 1(4):213–221. https://doi.org/10.1080/01431161.2010.481681

How Jin Aik D, Ismail MH, Muharam FM (2020) Land use/land cover changes and the relationship with land surface temperature using Landsat and MODIS imageries in Cameron Highlands. Malaysia Land 9(10):372. https://doi.org/10.3390/land9100372

Huang Q, Huang J, Yang X, Fang C, Liang Y (2019) Quantifying the seasonal contribution of coupling urban land use types on Urban Heat Island using land contribution index: a case study in Wuhan. China Sustain Cities Soc 44:666–675. https://doi.org/10.1016/j.scs.2018.10.016

Imhoff ML, Zhang P, Wolfe RE, Bounoua L (2010) Remote sensing of the urban heat island effect across biomes in the continental USA. Remote Sens Environ 114(3):504–513. https://doi.org/10.1016/j.rse.2009.10.008

Izrael Y, Hashimoto M, Tegart W (1990) Potential impacts of climate change. Report of IPCC Working Group II

Jabal ZK, Khayyun TS, Alwan IA (2022) Impact of climate change on crops productivity using MODIS-NDVI time series. Civ Eng J. https://doi.org/10.28991/CEJ-2022-08-06-04

Kadhim N, Ismael NT, Kadhim NM (2022) Urban landscape fragmentation as an indicator of urban expansion using sentinel-2 imageries. Civ Eng J 89:1799–1814. https://doi.org/10.28991/CEJ-2022-08-09-04

Karnieli A, Agam N, Pinker RT, Anderson M, Imhoff ML, Gutman GG, Panov N, Goldberg A (2010) Use of NDVI and land surface temperature for drought assessment: merits and limitations. J Central Banking Law Inst 23(3):618–633. https://doi.org/10.1175/2009JCLI2900.1

Kasap M (2017) Kayseri planla gelişen bir kent (mi)? Arkitera. https://www.arkitera.com/gorus/kayseri-planla-gelisen-bir-kent-mi/. Accessed 29 Dec 2022

Kayseri Büyükşehir Belediyesi (2019) 2020–2024 Stratejik kalkinma planı. Kayseri http://www.sp.gov.tr/upload/xSPStratejikPlan/files/sls36+kbb_stratejik_plan_2020_2024.pdf

Kayseri İl Tarım ve Orman Müdürlüğü (2022) Konum. https://kayseri.tarimorman.gov.tr/Menu/80/Cografi-Yapi#:~:text=Kayseri%20%C4%B0li%20370%2045'%20ve,ya%20karayoluyla%20316%20km%20uzakl%C4%B1ktad%C4%B1r. Accessed 25 Oct 2022

Ke X, Men H, Zhou T, Li Z, Zhu F (2021) Variance of the impact of urban green space on the urban heat island effect among different urban functional zones: a case study in Wuhan. Urban for Urban Green 62:127159. https://doi.org/10.1016/j.ufug.2021.127159

Khaliq A, Musci MA, Chiaberge M (2018) Analyzing relationship between maize height and spectral indices derived from remotely sensed multispectral imagery. In: 2018 IEEE Applied imagery pattern recognition workshop (AIPR)

Kim J-P, Guldmann J-M (2014) Land-use planning and the urban heat island. Environ Plann B Plann Des 41(6):1077–1099. https://doi.org/10.1068/b130091p

KTB (2022a) Coğrafi yapı. https://kayseri.ktb.gov.tr/TR-54966/cografi-yapi.html. Accessed 25 Oct 2022

KTB (2022b) Ekonomik yapı. T.C. Kültür ve Turizm Bakanlığı. https://kayseri.ktb.gov.tr/TR-55002/ekonomik-yapi.html#:~:text=T%C3%BCm%20bu%20geli%C5%9Fmelere%20kar%C5%9F%C4%B1n%20halk%C4%B1n,ve%20meyve%20%C3%BCretimi%20de%20yap%C4%B1l%C4%B1r. Accessed 25 Oct 2022

KTB (2022c) İklim ve bitki örtüsü. Kayseri İl Kültür ve Turizm Müdürlüğü. https://kayseri.ktb.gov.tr/TR-54978/iklim-ve-bitki-ortusu.html#:~:text=En%20s%C4%B1cak%20g%C3%BCnler%20Temmuz%20ve,C'a%20kadar%20d%C3%BC%C5%9Ft%C3%BC%C4%9F%C3%BC%20g%C3%B6r%C3%BClmektedir. Accessed 29 Oct 2022

Kumar BP, Babu KR, Anusha B, Rajasekhar M (2022) Geo-environmental monitoring and assessment of land degradation and desertification in the semi-arid regions using Landsat 8 OLI/TIRS, LST, and NDVI approach. Environ Chall 8:100578. https://doi.org/10.1016/j.envc.2022.100578Get

Li X, Zhou Y, Yu S, Jia G, Li H, Li W (2019) Urban heat island impacts on building energy consumption: a review of approaches and findings. Energy 174:407–419. https://doi.org/10.1016/j.energy.2019.02.183

Liu K, Su H, Li X, Wang W, Yang L, Liang H (2016) Quantifying spatial–temporal pattern of urban heat island in Beijing: An improved assessment using land surface temperature (LST) time series observations from LANDSAT, MODIS, and Chinese new satellite GaoFen-1. IEEE J Sel Top Appl Earth Obs Remote Sens 9(5):2028–2042. https://doi.org/10.1109/JSTARS.2015.2513598

Liu X, Ming Y, Liu Y, Yue W, Han G (2022) Influences of landform and urban form factors on urban heat island: Comparative case study between Chengdu and Chongqing. Sci Total Environ 820:153395. https://doi.org/10.1016/j.scitotenv.2022.153395

Lottering S, Mafongoya P, Lottering R (2022) Detecting and mapping drought severity using multi-temporal Landsat data in the uMsinga region of KwaZulu-Natal, South Africa. Geocarto Int 37(6):1574–1586. https://doi.org/10.1080/10106049.2020.1783580

Lowe SA (2016) An energy and mortality impact assessment of the urban heat island in the US. Environ Impact Assess Rev 56:139–144. https://doi.org/10.1016/j.eiar.2015.10.004

Lu Y, Feng X, Xiao P, Shen C, Sun J (2009) Urban heat island in summer of Nanjing based on TM data. In: Proceedings of the 2009 joint urban remote sensing event, Shanghai, China. https://doi.org/10.1109/URS.2009.5137628

Macarof P, Statescu F (2017) Comparasion of NDBI and NDVI as indicators of surface urban heat island effect in landsat 8 imagery: a case study of Iasi. Present Environm Sustain Dev 2:141–150. https://doi.org/10.1515/pesd-2017-0032

Mackey CW, Lee X, Smith RB (2012) Remotely sensing the cooling effects of city scale efforts to reduce urban heat island. Build Environ 49:348–358. https://doi.org/10.1016/j.buildenv.2011.08.004

Mallick J, Rahman A, Singh CK (2013) Modeling urban heat islands in heterogeneous land surface and its correlation with impervious surface area by using night-time ASTER satellite data in highly urbanizing city. Delhi-India Adv Space Res 52(4):639–655. https://doi.org/10.1016/j.asr.2013.04.025

Meng Q, Liu W, Zhang L, Allam M, Bi Y, Hu X, Gao J, Hu D, Jancsó T (2022) Relationships between land surface temperatures and neighboring environment in highly urbanized areas: seasonal and scale effects analyses of Beijing. China Remote Sens 14(17):4340. https://doi.org/10.3390/rs14174340

Ministry of Environment and Urbanization (2020) Environmental problems and priorities assessment report of Turkey. Ankara, Türkiye: Ministry of Environment and Urbanization https://webdosya.csb.gov.tr/db/ced/icerikler/tu-rk-yecevresorunlariveoncel-kler-_2020-20210401124420.pdf

Mirzaei PA (2015) Recent challenges in modeling of urban heat island. Sustain Cities Soc 19:200–206. https://doi.org/10.1016/j.scs.2015.04.001

Norton BA, Coutts AM, Livesley SJ, Harris RJ, Hunter AM, Williams NS (2015) Planning for cooler cities: a framework to prioritise green infrastructure to mitigate high temperatures in urban landscapes. Landsc Urban Plan 134:127–138. https://doi.org/10.1016/j.landurbplan.2014.10.018

O'Malley C, Piroozfar P, Farr ER, Pomponi F (2015) Urban heat island (UHI) mitigating strategies: a case-based comparative analysis. Sustain Cities Soc 19:222–235. https://doi.org/10.1016/j.scs.2015.05.009

Ozenen Kavlak M, Cabuk SN, Cetin M (2021) Development of forest fire risk map using geographical information systems and remote sensing capabilities: Ören case. Environ Sci Pollut Res 28(25):33265–33291. https://doi.org/10.1007/s11356-021-13080-9

Palme M, Inostroza L, Villacreses G, Lobato-Cordero A, Carrasco C (2017) From urban climate to energy consumption. Enhancing building performance simulation by including the urban heat island effect. Energy Build 145:107–120. https://doi.org/10.1016/j.enbuild.2017.03.069

Prasad S, Singh R (2022) Urban heat island (UHI) Assessment using the satellite data: a case study of Varanasi city, India. In: Smart cities for sustainable development. pp. 287–299. Springer. https://doi.org/10.1007/978-981-16-7410-5_17

Rizwan AM, Dennis LY, Chunho L (2008) A review on the generation, determination and mitigation of urban heat island. J Environ Sci 20(1):120–128. https://doi.org/10.1016/S1001-0742(08)60019-4

Rousta I, Sarif MO, Gupta RD, Olafsson H, Ranagalage M, Murayama Y, Zhang H, Mushore TD (2018) Spatiotemporal analysis of land use/land cover and its effects on surface urban heat island using Landsat data: a case study of Metropolitan City Tehran (1988–2018). Sustainability 10(12):4433. https://doi.org/10.3390/su10124433

Sheng L, Tang X, You H, Gu Q, Hu H (2017) Comparison of the urban heat island intensity quantified by using air temperature and Landsat land surface temperature in Hangzhou. China Ecol Indic 72:738–746. https://doi.org/10.1016/j.ecolind.2016.09.009

Shishegar N (2014) The impact of green areas on mitigating urban heat island effect: a review. Int J Environ Sustain 9(1):119–130. https://doi.org/10.18848/2325-1077/CGP/v09i01/55081

Silva JS, da Silva RM, Santos CAG (2018) Spatiotemporal impact of land use/land cover changes on urban heat islands: a case study of Paço do Lumiar. Brazil Build Environ 136:279–292. https://doi.org/10.1016/j.buildenv.2018.03.041

Singh R, Grover A (2015) Spatial correlations of changing land use, surface temperature (UHI) and NDVI in Delhi using Landsat satellite images. In: Urban Development Challenges, Risks and Resilience in Asian Mega Cities, (pp. 83–97). Springer

Steeneveld G-J, Koopmans S, Heusinkveld B, Van Hove L, Holtslag A (2011) Quantifying urban heat island effects and human comfort for cities of variable size and urban morphology in the Netherlands. J Geophys Res Atmos. https://doi.org/10.1029/2011JD015988

Sun S, Xu X, Lao Z, Liu W, Li Z, García EH, He L, Zhu J (2017) Evaluating the impact of urban green space and landscape design parameters on thermal comfort in hot summer by numerical simulation. Build Environ 123:277–288. https://doi.org/10.1016/j.buildenv.2017.07.010

Sun T, Sun R, Chen L (2020) The trend inconsistency between land surface temperature and near surface air temperature in assessing urban heat island effects. Remote Sens 12(8):1271. https://doi.org/10.3390/rs12081271

Sun L, Gao F, Xie D, Anderson M, Chen R, Yang Y, Yang Y, Chen Z (2021) Reconstructing daily 30 m NDVI over complex agricultural landscapes using a crop reference curve approach. Remote Sens Environ 253:112156. https://doi.org/10.1016/j.rse.2020.112156

Taleghani M (2018) Outdoor thermal comfort by different heat mitigation strategies-a review. Renew Sust Energ Rev 81:2011–2018. https://doi.org/10.1016/j.rser.2017.06.010

Taloor AK, Manhas DS, Kothyari GC (2021) Retrieval of land surface temperature, normalized difference moisture index, normalized difference water index of the Ravi basin using Landsat data. Appl Comput Geosci 9:100051. https://doi.org/10.1016/j.acags.2020.100051

Talukdar S, Rihan M, Hang HT, Bhaskaran S, Rahman A (2022) Modelling urban heat island (UHI) and thermal field variation and their relationship with land use indices over Delhi and Mumbai metro cities. Environ Dev Sustain 24(3):3762–3790. https://doi.org/10.1007/s10668-021-01587-7

Tian P, Li J, Cao L, Pu R, Wang Z, Zhang H, Chen H, Gong H (2021) Assessing spatiotemporal characteristics of urban heat islands from the perspective of an urban expansion and green infrastructure. Sustain Cities Soc 74:103208. https://doi.org/10.1016/j.scs.2021.103208

Vailshery LS, Jaganmohan M, Nagendra H (2013) Effect of street trees on microclimate and air pollution in a tropical city. Urban for Urban Green 12(3):408–415. https://doi.org/10.1016/j.ufug.2013.03.002

Kayseri Valiliği (2022a) Kayseri. http://www.kayseri.gov.tr/ilcelerimiz. Accessed 25 Oct 2022

Kayseri Valiliği (2022b) Nüfus ve idari yapı. http://www.kayseri.gov.tr/nufus-durumu. Accessed 25 Oct 2022

Venter ZS, Krog NH, Barton DN (2020) Linking green infrastructure to urban heat and human health risk mitigation in Oslo. Norway Sci Total Environ 709:136193. https://doi.org/10.1016/j.scitotenv.2019.136193

Wang J, Huang B, Fu D, Atkinson PM, Zhang X (2016) Response of urban heat island to future urban expansion over the Beijing–Tianjin–Hebei metropolitan area. Appl Geogr 70:26–36. https://doi.org/10.1016/j.apgeog.2016.02.010

Weng Q, Fu P, Gao F (2014) Generating daily land surface temperature at Landsat resolution by fusing Landsat and MODIS data. Remote Sens Environ 145:55–67. https://doi.org/10.1016/j.rse.2014.02.003

Yao L, Li T, Xu M, Xu Y (2020) How the landscape features of urban green space impact seasonal land surface temperatures at a city-block-scale: an urban heat island study in Beijing. China Urban for Urban Green 52:126704. https://doi.org/10.1016/j.ufug.2020.126704

Yuan X, Wang W, Cui J, Meng F, Kurban A, De Maeyer P (2017) Vegetation changes and land surface feedbacks drive shifts in local temperatures over Central Asia. Sci Rep 7(1):1–8

Zha Y, Gao J, Ni S (2003) Use of normalized difference built-up index in automatically mapping urban areas from TM imagery. Int J Remote Sens 24(3):583–594. https://doi.org/10.1080/01431160304987

Zhao L, Lee X, Smith RB, Oleson K (2014) Strong contributions of local background climate to urban heat islands. Nature 511(7508):216–219. https://doi.org/10.1038/nature13462

Zhou W, Huang G, Cadenasso ML (2011) Does spatial configuration matter? Understanding the effects of land cover pattern on land surface temperature in urban landscapes. Landsc Urban Plan 102(1):54–63. https://doi.org/10.1016/j.landurbplan.2011.03.009

Zoran M, Savastru R, Savastru D, Tautan MN, Dida MR (2011) Satellite observation of urban heat island effect. In: Proceedings of the global conference on global warming, Lisbon, Portugal

Zou Z, Yan C, Yu L, Jiang X, Ding J, Qin L, Wang B, Qiu G (2021) Impacts of land use/land cover types on interactions between urban heat island effects and heat waves. Build Environ 204:108138. https://doi.org/10.1016/j.buildenv.2021.108138

Authors and Affiliations

Mehmet Cetin[1] · Mehtap Ozenen Kavlak[2] · Muzeyyen Anil Senyel Kurkcuoglu[3] · Gulsah Bilge Ozturk[4] · Saye Nihan Cabuk[5] · Alper Cabuk[6]

✉ Mehmet Cetin
mehmet.cetin.landscape.architect@gmail.com; mehmet.cetin@omu.edu.tr

[1] Present Address: Department of City and Regional Planning, Faculty of Architecture, Ondokuz Mayis University, 55200 Samsun, Turkey

[2] Department of Remote Sensing and Geographical Information Systems, Institute of Graduate Programs, Eskisehir Technical University, 26555 Eskisehir, Turkey

[3] Department of City and Regional Planning, Faculty of Architecture, Middle East Technical University, 06800 Ankara, Turkey

[4] Department of Landscape Architecture, Faculty of Agriculture, Ordu University, 52200 Ordu, Turkey

[5] Department of Geodesy and Geographical Information Technologies, Institute of Earth and Space Sciences, Eskisehir Technical University, 26555 Eskisehir, Turkey

[6] Department of Architecture, Faculty of Architecture and Design, Eskisehir Technical University, 26555 Eskisehir, Turkey